

# An Updated Surface Gravity Prediction Model (xGRAV20)

Kevin AHLGREN, United States

**Key words:** Vertical reference systems, Gravity, Geoid

## SUMMARY

The National Oceanic and Atmospheric Administration's (NOAA) National Geodetic Survey (NGS) is modernizing a number of products and models that support the future datum in North America – the North American-Pacific Geopotential Datum 2022 (NAPGD2022). This paper will focus on the newly released experimental surface gravity model, xGRAV20. This is the initial BETA release of what ultimately will be an official surface gravity model, GRAV2022.

The xGRAV20 model is based on approximately 10 million terrestrial gravity observations and a high resolution digital elevation model (DEM). The model can be used for estimating geodetic leveling corrections and other geodetic and geophysical applications where an absolute gravimeter is not available. This paper will highlight the model methodology and will present an external validation using independent, high-accuracy absolute gravity data acquired by the NGS Geoid Slope Validation Surveys in Texas, Iowa, and Colorado. Two additional elements will also be investigated in this paper: 1) the estimated uncertainty of the surface gravity model, and 2) the impact that new terrestrial gravity data has on omission error.

Overall results show that the xGRAV20 model is very consistent with published geoid accuracies (Smith et al., 2013, Wang et al., 2017, van Westrum et al., 2021). In Texas (with no topography and a relatively smooth gravity field), the gravity model is accurate to ~0.75 mGal (RMS). In more difficult gravity fields like those present in Iowa and Colorado, the xGRAV20 model shows accuracies at 1.6 mGal and 1.85 mGal, respectively. Geoid accuracies are approximately 1 cm, 1.5 cm, and 3.6 cm for Texas, Iowa, and Colorado, respectively.

Additionally over Iowa, we illustrate the impact that the observational noise and new data can have on the model results. From these tests, it is quite possible that the current noise estimates are too conservative in this region; and the model shows improvement at the 0.5 mGal (RMS) level when a new gravity dataset is incorporated.

# An Updated Surface Gravity Prediction Model (xGRAV20)

Kevin AHLGREN, United States

## 1. INTRODUCTION

NGS is in the process of modernizing the National Spatial Reference System (NSRS); like a lot of countries throughout the world, NGS is using a geoid model as the basis for the vertical reference system. One component of the modernized NSRS and vertical datum is a surface gravity model, which will provide a full-field gravity value at the Earth's surface for any location within the NSRS region. The initial and experimental model, xGRAV20, will be presented and discussed in this paper. This model is available for public BETA testing at the following NGS website: <https://beta.ngs.noaa.gov/GEOID/xGRAV20/index.shtml>.

The xGRAV20 model relies on a vast amount of historical terrestrial gravity data of roughly 10 million points including altimetry derived observations over the oceanic regions. In addition to the gravity data, a DEM is needed to ‘restore’ the anomaly field back to a full-field amount. While the data components were covered previously (Ahlgren and Krcmaric, 2020), a brief description of the methodology and covariance function used is provided in Section 2. In Section 3, results are shown compared to the GSVS lines in Texas, Iowa, and Colorado. A more in-depth investigation is shown for the GSVS14 line over Iowa which includes a number of different observational noise scenarios and the inclusion of new terrestrial gravity data. Both of these changes can be quite impactful on the model results.

## 2. xGRAV20 METHODOLOGY

The gravity prediction scheme employed by the xGRAV20 tool relies on the refined Bouger anomaly at point-level (Ahlgren and Krcmaric, 2020). However, a few adaptations to this method are presented in the following section to highlight the exact procedure. The xGRAV20 model also suffers from some inconsistencies due to the terrain correction and atmospheric correction at sub-mGal levels. These improvements will be included in a future xGRAV model.

The covariance function used in the model for interpolation purposes is described in Section 2.1. Due to operational and computational requirements, intermediate data types are pre-computed on regular grids as discussed in Section 2.2. Additionally, the error estimation is presented in Section 2.3. The error estimation is not currently released in the xGRAV20 model but future xGRAV models will incorporate this information.

### 2.1 Covariance Function Parameters

The covariance function used is shown in (1) and is based on a three-dimensional logarithmic function (Forsberg, 1987) that uses location specific parameters ( $D$  and  $T$ ) depending on the existing surface gravity data.

$$C(p^{H_1}, q^{H_2}) = -f \sum_{i=0}^3 \alpha_i \log(z + r) \quad (1)$$

where:

$f = C_0 / \log\left(\frac{D_1^3 D_3}{D_0 D_2^3}\right)$ , with  $D_i = D + iT$  and  $C_0$  as the variance.

$\alpha_0 = 1; \alpha_1 = -3; \alpha_2 = 3; \alpha_3 = -1;$

$z = H_1 + H_2 + D_i; r = \sqrt{(x_2 - x_1)^2 + (y_2 - y_1)^2 + z^2}$

## 2.2 Intermediate Gridded Data

The applied method of gravity prediction is very computationally time-consuming especially with respect to terrain corrections. While a single prediction point takes a few seconds, the implementation on an entire leveling line of 100s of points would simply take too long and be poor customer service. With this in mind, the xGRAV20 model relies on pre-computed, gridded data that is simply interpolated at the user-specified location. The specifications for each intermediate data type are shown in Table 1.

Table 1: Specifications for gridded data types used in xGRAV20:

Data Type:	Spatial Resolution:
Digital Elevation Model	3"
Refined Bouguer Anomaly	1'
Terrain Correction	15"

At a user specified location ( $\varphi, \lambda, H$  (optional)), the estimated full field gravity value ( $\hat{g}$ ) will be calculated by the tool based on (2).

$$\hat{g} = \widehat{\Delta g} + \frac{dy}{dh} H + \frac{1}{2} \frac{d^2 \gamma}{dh^2} H^2 + \gamma - \delta g_{ATM} + 0.11195H - A \quad (2)$$

where:

$\widehat{\Delta g}$  = interpolated refined Bouguer anomaly from 1' grid pre-computed on the Earth's surface

$H$  = user specified elevation (or interpolated from 3" DEM)

$$\gamma = \frac{a\gamma_a \cos^2 \varphi + b\gamma_b \sin^2 \varphi}{\sqrt{a^2 \cos^2 \varphi + b^2 \sin^2 \varphi}}; \frac{dy}{dh} = \frac{-2\gamma}{a}(1 + f + m - 2f \sin^2 \varphi); \frac{d^2 \gamma}{dh^2} = \frac{6\gamma}{a}$$

$\gamma_a, \gamma_b, a, b, f, m$  are all parameters from the GRS80 reference ellipsoid

$$\delta g_{ATM} = 0.87 * e^{-0.116*(H/1000)^{1.047}}$$

$A$  = standard terrain correction with density of 2.67 g/cm<sup>3</sup> interpolated from 15" grid

## 2.3 Error Estimation

While the estimated uncertainty is currently not included in xGRAV20, a brief discussion is presented here to provide context for future models. Any error in the terms of (2) will

propagate into the estimated uncertainty for the gravity value. The majority of the estimated uncertainty comes from the refined Bouguer anomaly and can be estimated according to (3) from Moritz (1980) with covariance functions consistent with (1) from Forsberg (1987).

$$\widehat{\sigma_{RBA}^2} = C_{ss} - C_{st}(C_{tt} + C_{nn})^{-1}C_{ts} \quad (3)$$

where:

$C_{ss}$  = autocovariance of  $s$ , which are the points being predicted

$C_{tt}$  = autocovariance of  $t$ , which are the points being used in the prediction

$C_{st}$  &  $C_{ts}$  = cross-covariance between  $s$  &  $t$  and vice versa

$C_{nn}$  = observational noise variance

The  $C_{nn}$  term is based on an estimated uncertainty associated with each terrestrial gravity observation and the impact of this will be highlighted in Section 3.1.2.

The other major contributor to the estimated uncertainty comes from the uncertainty in the elevation,  $H$ . The combined effect of this term is approximately  $0.1967 * \sigma_H$ .

We acknowledge that additional uncertainty contributions from the atmospheric correction and the terrain correction exist – however, these contributions are not discussed any further. The atmospheric component is fairly minor at only about 0.01 mGal per 100 meter of height error. The terrain correction component will mostly be accounted for with consistent handling in the remove-restore steps with any remaining error coming from interpolation errors.

### 3. RESULTS

In the following section, model results in terms of the actual gravity field estimation and its estimated uncertainty are presented for three regions in the United States: Iowa (GSVS14), Texas (GSVS11), and Colorado (GSVS14). These three regions include a GSVS profile that can be used as ground validation when compared with the gravity prediction results. More information about the GSVS lines is available at the associated references (Smith et al., 2013; Wang et al., 2017; van Westrum et al., 2021).

#### 3.1 GSVS14

A greater focus is put on this region in Iowa in this paper due to two factors: 1) it is probably the most difficult region to predict gravity due to the large gravity signal from a rifting event and lack of terrestrial gravity data and 2) a new terrestrial gravity survey was performed by USGS (Reitman and Drenth, 2019) allowing us to highlight the impact of adding new data to the prediction. The general region is shown in Figure 1 with the refined Bouguer anomaly predicted over a 1' grid for the various scenarios discussed below.

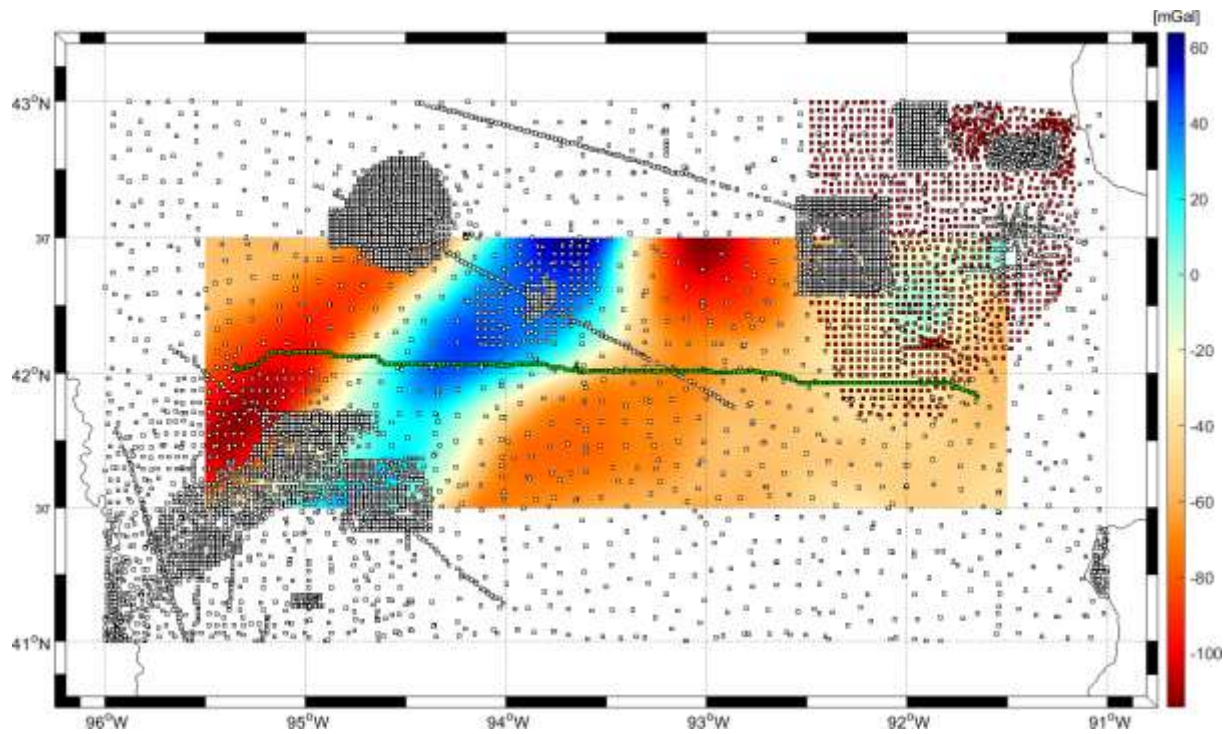


Figure 1: GSVS14 Region with refined Bouguer anomaly in mGal. White squares are existing terrestrial gravity data used in the xGRAV20 model; Red squares are new terrestrial gravity observations from USGS (Reitman and Drenth, 2019); Green squares are the GSVS14 ground truth data.

### 3.1.1 Covariance Parameter Estimation

To get a deeper perspective on the covariance model used in this prediction scheme, the estimated covariance function parameters,  $D$  and  $T$ , (from (1)) are illustrated in Figure 2 and 3, respectively. These are based on the original terrestrial gravity dataset and are geographically variable based on the underlying data.

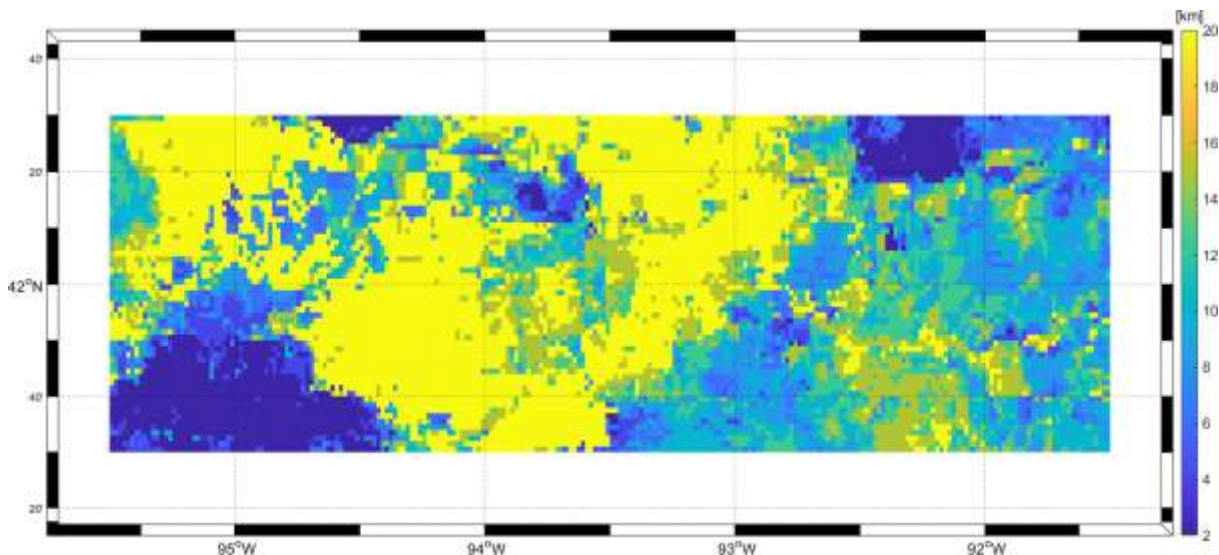


Figure 2:  $D$  estimated covariance parameter [km].

The  $D$  term is impacted by the density of the underlying data and the magnitude of the signal predicted. In regions where the underlying data is dense, the  $D$  term is smaller as can be seen in the southwest portion of Figure 2. Additionally, the larger magnitude in the gravity field in the western two-thirds of the region will generally cause the  $D$  term to be larger compared to the eastern one-third where the magnitude of the field and the  $D$  term are both smaller.

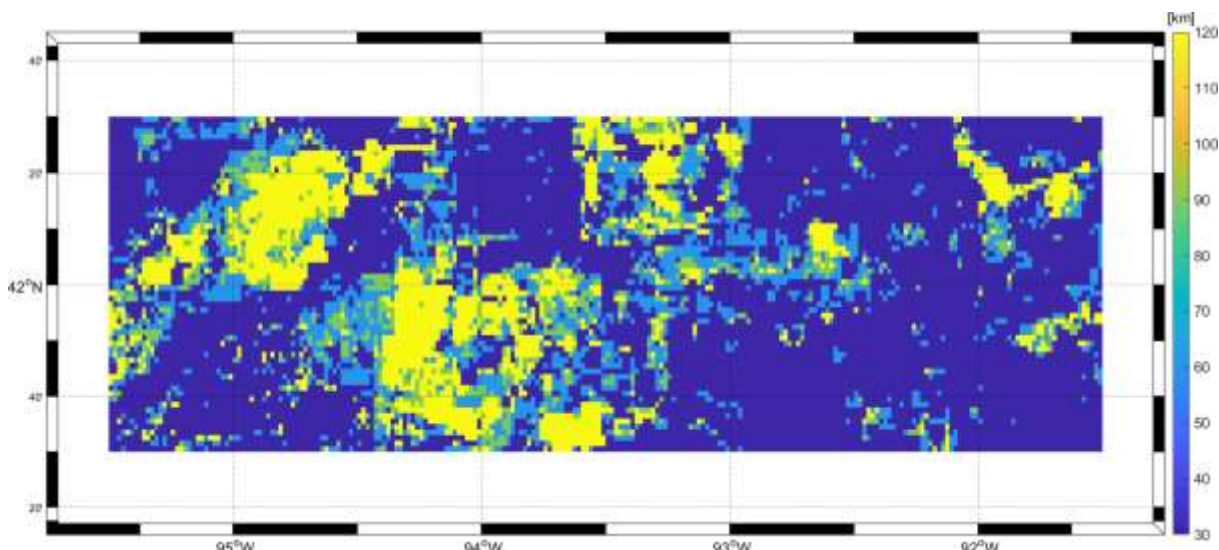


Figure 3:  $T$  estimated covariance parameter [km].

The  $T$  term shown in Figure 3 is generally impacted by the same two factors: data density and signal magnitude. However, this term is more impacted by the horizontal gradient of the field than the magnitude. There is considerably less coherence with this term compared to the  $D$  term, which will be the subject of future investigation.

### 3.1.2 Impact of different observational noise scenarios

While often overlooked, the observational noise associated with each underlying data point has a significant impact on the predictions. This is important because we don't have additional information about how the terrestrial gravity surveys were performed that would include realistic gravity uncertainties. This is a very common scenario in many countries that rely on decades-old gravity datasets. As a consequence, we utilize an estimated uncertainty on each underlying gravity observation, which is used as the diagonal elements of  $C_{nn}$  in (3). This original scenario is shown as Case I in the following section.

To highlight the importance of this observational noise, we estimate the gravity field with two additional noise scenarios keeping everything else the same: 1) original noise from Case I is reduced by a factor of 2 resulting in Case II; and 2) noise is fixed to a constant value of 1 mGal for all points resulting in Case III. The comparison of these three cases to the ground truth data collected with the GSVS14 survey is illustrated in Figure 4 along with statistics in Table 2.

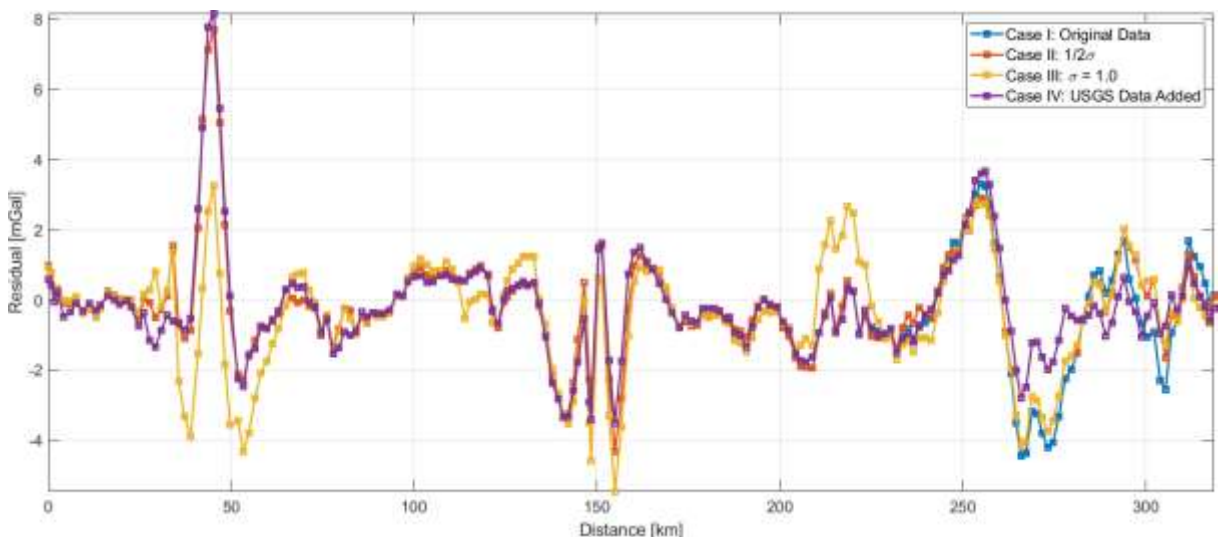


Figure 4: GSVS14 gravity prediction residuals. Case I: original noise; Case II: noise is 1/2 that of Case I; Case III: uniform noise of 1.0 mGal; Case IV: new USGS data added (see Section 3.1.3 for details). Direction of profile is west to east.

Table 2: GSVS14 gravity prediction residual statistics.

	Min. [mGal]	Max. [mGal]	Mean [mGal]	Std. Dev. [mGal]	RMS [mGal]	Skewness [ ]	Kurtosis [ ]
Case I	-4.44	8.16	-0.26	1.70	1.72	1.09	8.37
Case II	-4.32	7.70	-0.19	1.59	1.60	1.01	8.29
Case III	-5.45	3.27	-0.39	1.57	1.62	-0.59	3.49
Case IV	-3.50	8.16	-0.17	1.52	1.53	1.95	11.29

Isolating our comparison to Cases I, II, and III for the moment, it is evident that Case II and Case III are superior to Case I, which signifies that the original noise estimates are likely too

conservative. However, caution should be exercised as we have very sparse data in this region and the models are only different in a few areas of the GSVS14 profile (see Figure 4 around 45 km, 125 km, and 220 km).

It is possible that only a small handful of points have unrealistic, conservative noise estimates. For example, the region from 30 to 65 km is illustrated in Figure 5 with the observational standard deviations shown. At approximately 40 km and again at 50 km, there are two individual observations that have an estimated noise of 10 mGal, which based on the preceding results seems too conservative and is degrading the results to some degree.

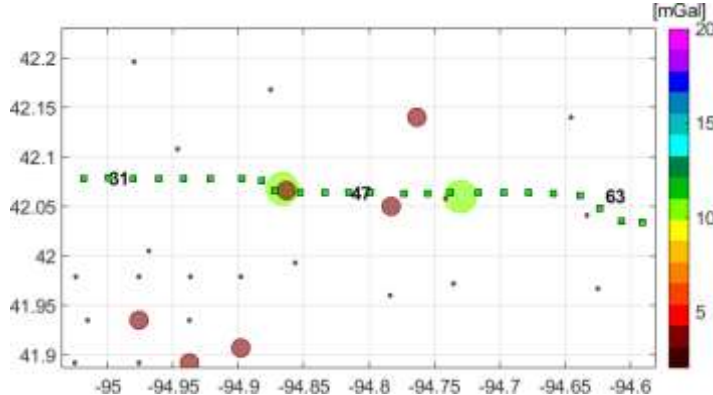


Figure 5: GSVS14 profile from 30 km to 65 km with estimated noise (standard deviations) in mGal. Numbers in bold are the distance along the GSVS14 profile from the west end. Green squares are the GSVS14 validation data locations.

In order to provide a little more detail about the various cases, each model residual is shown in Figure 6 as the total percentage of points below a particular threshold from the GSVS14 data: 0.5 mGal, 1 mGal, 2 mGal, and 5 mGal. This removes the impact of large residuals that have more influence on the standard deviation and RMS shown in Table 2. Based on Figure 6, it is evident that Case II is outperforming Case I and Case III with significantly higher percentages of data within 0.5 mGal, 1 mGal, and 2 mGal. One other significant conclusion from Figure 4 and Figure 6 is that we likely would have incorrectly identified Case III as the best scenario, if we would have only considered Figure 4 (Case III has the lowest std. dev., best handling of large residuals (tight min. to max and kurtosis near 3)). However, Figure 6 illustrates support for Case II being a more accurate model.

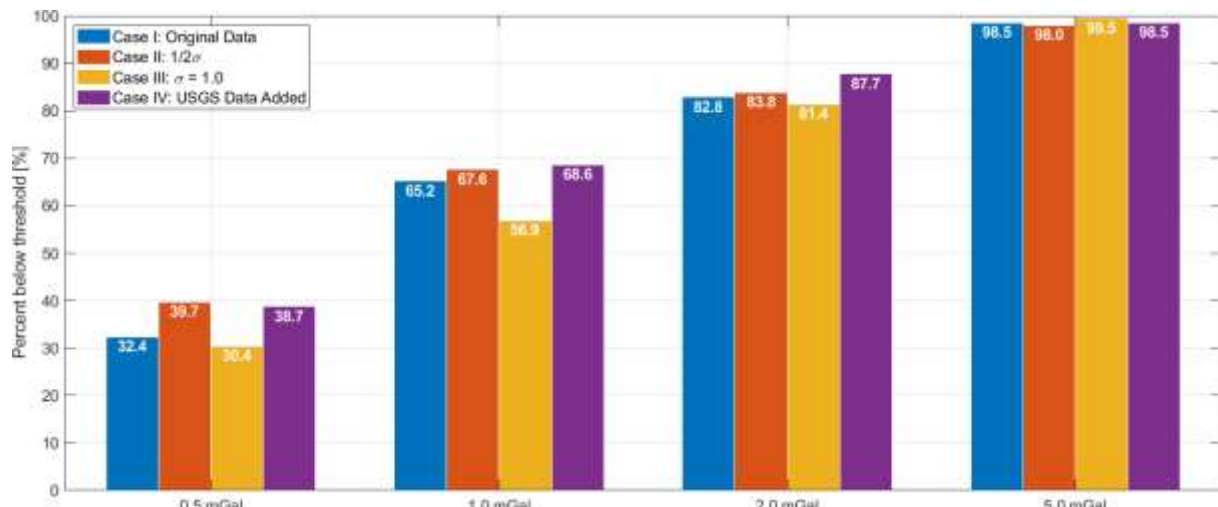


Figure 6: Percentage of data where the gravity residual to GSVS14 is below a particular threshold (0.5, 1.0, 2.0, & 5.0 mGal).

Finally, the Case I estimated model uncertainties are shown in Figure 7. The model uncertainties are impacted mostly by data density and are typically at the 1.5 mGal level though they can approach almost 9 mGal in a worst-case scenario.

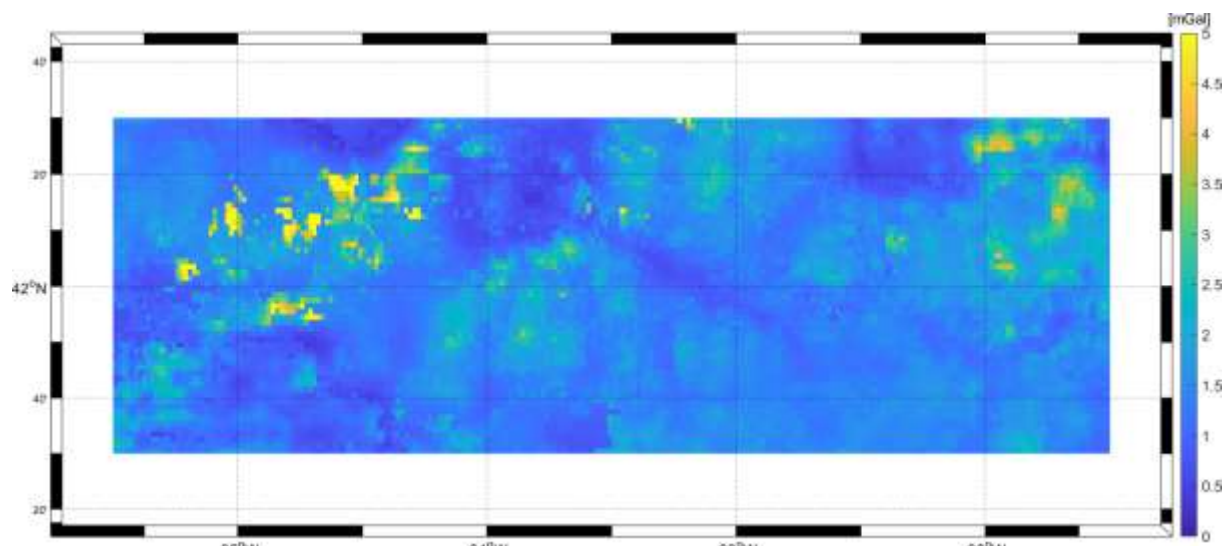


Figure 7: Case I estimated uncertainty at 1-sigma. Statistics in [mGal]: [Min: 0.32; Max: 8.87; Mean: 1.48; Std. Dev.: 0.61]

Additionally, the error envelope is shown along the GSVS14 profile for Case I, II, and III in Figure 8. This signifies how frequently the model is within the estimated uncertainties, so if any given observation is within the envelope, it is within the 1-sigma level for that particular model. Figure 8 shows consistent results as those presented in Figure 4. Table 3 shows the percentage of data from each case that falls within the 1-sigma level and 1.96-sigma level, which under ideal, normal distribution should be 68% and 95%, respectively. This highlights a slightly different result in that the error envelope is more realistic with the initial, Case I, observational noise estimates.

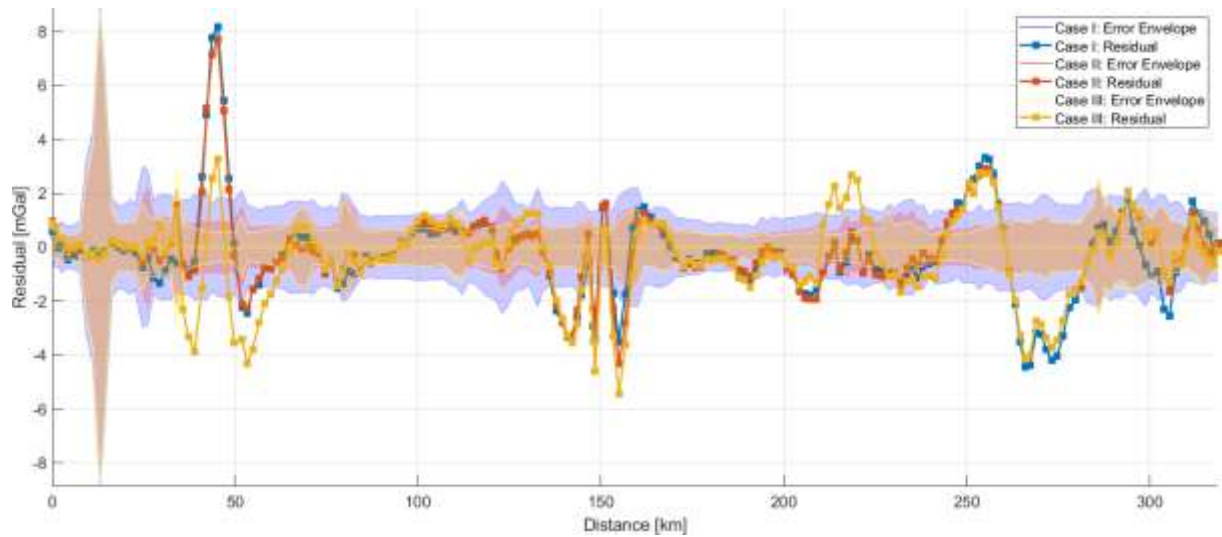


Figure 8: Case I, II, and III model residual profiles compared with GSVS14 with 1-sigma error envelope shown.

Table 3: Percentage of data within error envelope(s)

	<i>Percentage within 1-sigma estimate</i>	<i>Percentage within 1.96-sigma estimate</i>
Case I	73.0	91.7
Case II	54.4	77.9
Case III	46.6	70.1
Case IV	77.5	92.6

### 3.1.3 Impact of new terrestrial gravity data on results

Finally, results from Case IV are presented in the following section. In this case, a new terrestrial gravity dataset collected by the USGS from 2016 to 2018 (Reitman and Drenth, 2019) is incorporated to the original underlying dataset and used in the model predictions. This dataset has 1080 observations, which are given an assumed noise of 2 mGal on each observation, which is likely too conservative, but is consistent with the minimum noise in the original data. These results are shown in Figure 4 and 6 along with Table 2. This case is identical to Case I up to the ~225 km distance. From ~225 km to the end of the GSVS14 profile, the new data improves the results quite significantly and decreases the overall RMS from 1.72 mGal (Case I) to 1.53 mGal (Case IV). However, if we isolate just the section being impacted by the new data (the last 74 observations – from 225 km to the end), the RMS drops from 1.86 mGal to 1.35 mGal (i.e. 0.5 mGal improvement) with the new data. The error envelope for Case IV is shown in Figure 9 where the improvement is clearly visible along with an overall decrease in the estimated uncertainty from ~225 km to the end of the profile.

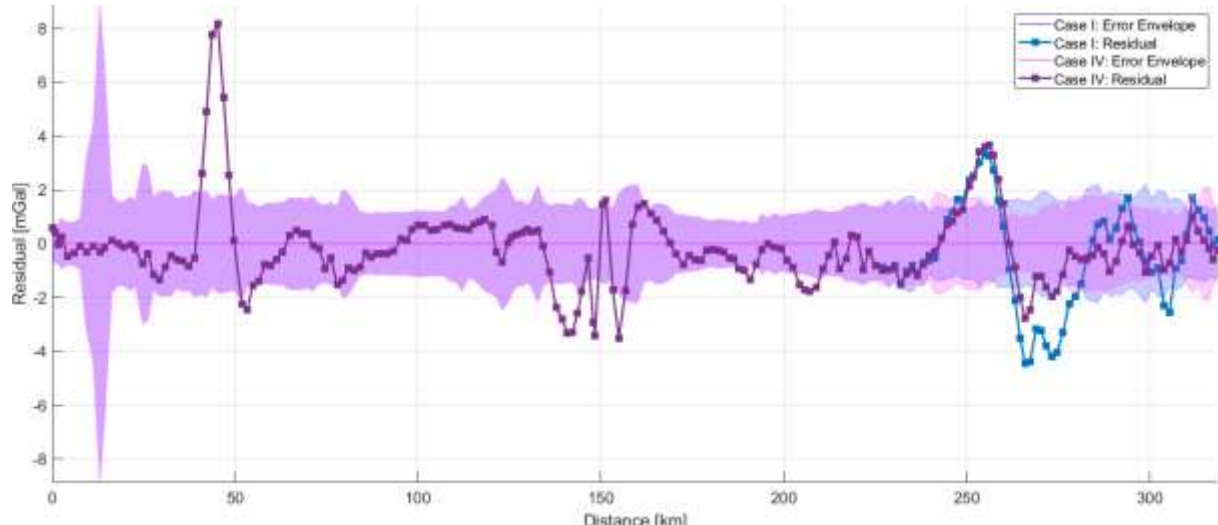


Figure 9: Case I and IV model residual profiles compared with GSVS14 with 1-sigma error envelope shown.

### 3.2 GSVS11

A more concise overview of the results of an update to the xGRAV20 model over the Texas GSVS11 region and is presented in the following section. These results are slightly different than those obtained from the publically available version as the terrain correction and atmospheric correction are modified slightly. The model residuals compared with the GSVS11 validation data are shown in Figure 10.

The gravity field in this region is much more consistent than either of the other two regions and this is evident in the results as predictions are accurate at the 0.75 mGal RMS level. The first 100 km of the profile has slightly degraded performance compared to the rest of the profile.

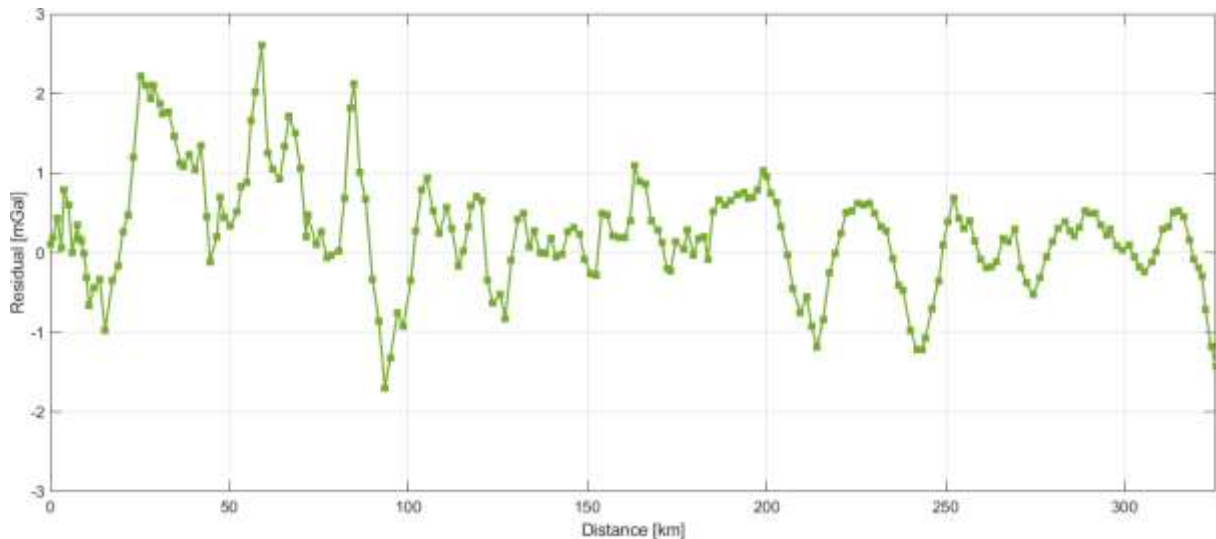


Figure 10: Gravity model estimate residuals from GSVS11. Residual statistics in [mGal]: [Min: -1.70; Max: 2.61; Mean: 0.27; Std. Dev.: 0.71; RMS: 0.76; Skewness: 0.37; Kurtosis: 3.99]. Direction of profile is north to south.

### 3.3 GSVS17

The updated gravity model results over the mountainous Colorado region are shown in Figure 11 along with the elevation profile for added context as this profile has extreme elevation differences (from 1900 to 3300 meters). Overall, the model performs quite well with 1.84 mGal RMS. Over the first 2/3 of the profile (from 0 km to 240 km), the model performs very well with residuals rarely exceeding +/- 2 mGals. However, from 240 km to 315 km, which coincides with the second mountain pass, there is a more significant degradation in the results with residuals at the 4 to 6 mGal level. This section has very limited gravity coverage, which also has significant ramifications for geoid modeling. This is evident in Wang et al (2021) where 14 independent geoid models all diverge from the ground truth by 5 to 10 cm in this same section.

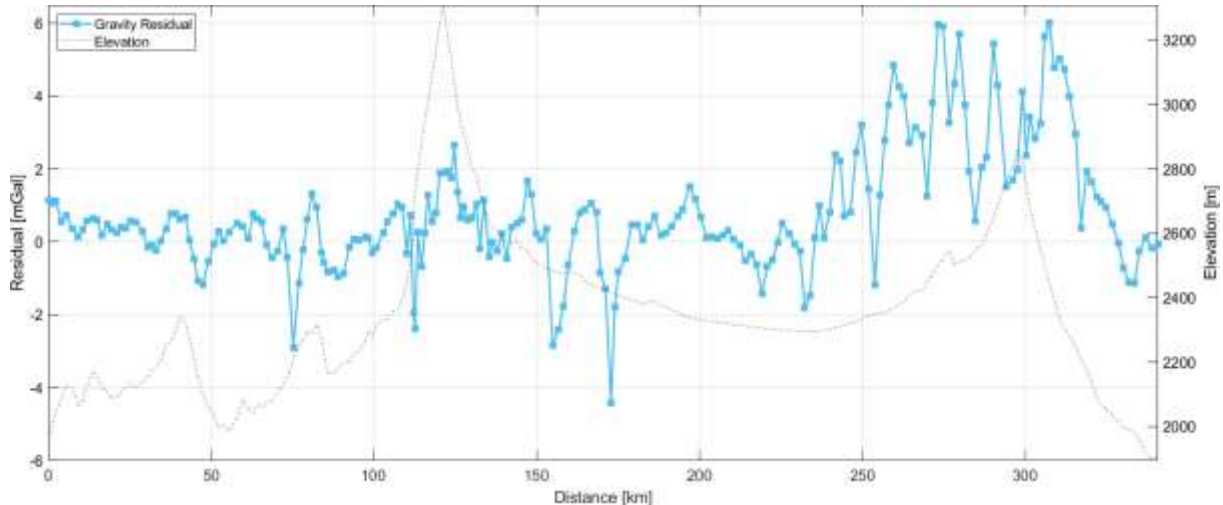


Figure 11: Gravity model estimate residuals from GSVS17 (in cyan) with elevation profile (in black) for context. . Residual statistics in [mGal]: [Min: -4.41; Max: 6.01; Mean: 0.77; Std. Dev.: 1.66; RMS: 1.84; Skewness: 0.96; Kurtosis: 4.71]. Direction of profile is west to east.

## 4. CONCLUSION

Overall, the xGRAV20 model provides a computationally fast and accurate surface gravity value over the NAPGD2022 region. This model is based on the refined Bouguer gravity anomaly and a three-dimensional logarithmic covariance function that has been pre-computed on a 1' grid. This paper highlights the results of the estimated uncertainties that are not currently a part of xGRAV20 but will be included in a future model.

The covariance function employed by xGRAV20 estimates two geographically variable parameter ( $D$  and  $T$ ) that are influenced by the density of the surrounding underlying gravity data, the magnitude of the gravity field, and the variability of the gravity field. For the GSVS14 region over Iowa, the  $D$  parameter is almost completely controlled by the data density and the  $T$  parameter is influenced by a more complex combination of these properties.

Additionally, there is clearly an importance from the observational noise estimates that is often overlooked. Over the GSVS14 region, three scenarios (Case I, II, & III) were shown where only the observational noise was altered. Based on these scenarios, it is likely that the noise estimates currently used in xGRAV20 are too conservative or a small number of observations have too conservative noise values. From these scenarios, we also see the importance of using additional statistics when evaluating statistical results.

The final conclusion from the GSVS14 test cases is the importance of new gravity data. While this isn't a surprising conclusion, the incorporation of new, high accuracy terrestrial gravity data will very likely lead to improved results and drive down uncertainty estimates. This is especially true in the GSVS14 region where the data distribution is quite sparse and we see improvements of 2+ mGals on individual marks and 0.5 mGal RMS overall (the last 74 observations that are influenced by the new data have 1.35 mGal RMS with new data compared to 1.86 mGal RMS, originally).

The gravity prediction results shown here are very consistent with the geoid results that have been reported on the GSVS lines. Over GSVS11, Smith et al (2013) report +/- 1 cm relative geoid errors which is in line with the +/- 1.1 cm standard deviation error obtained with xGEOID20B. Over this region, the gravity is approximately +/- 0.75 mGal RMS based on results presented in this paper. Over GSVS14, Wang et al (2017) report +/- 1.5 cm geoid error; results presented in Section 3.1 for the gravity field show accuracies at the ~1.6 mGal level. For GSVS17, van Westrum et al (2021) show results of +/- 3.6 cm for the geoid profile which is consistent with results for the gravity field of 1.84 mGal presented in Section 3.3.

There are still areas for improvement that a future xGRAV model will incorporate. Realistic error estimates need to be determined and included in the model as evidenced by Section 3. More consistent terrain and atmospheric corrections will lead to sub-mGal improvements; however, more impactful improvements can likely be achieved with observational noise estimates that are more realistic, better outlier and suspect data detection and handling, and more accurate data in gap areas.

## REFERENCES

- Ahlgren, K. and Krcmaric, J. (2020). The NGS Surface Gravity Prediction Tool. FIG Working Week 2020 Proceedings.
- Forsberg, R. (1987). A new covariance model for inertial gravimetry and gradiometry. *Journal of Geophysical Research: Solid Earth*, 92(B2), 1305-1310.
- Moritz, H. (1980). Advanced Physical Geodesy. Herbert Wichmann, Karlsruhe.
- Reitman, J.J., and Drenth, B.J. (2019). Principal facts of regional gravity data in northeast Iowa: U.S. Geological Survey data release, <https://doi.org/10.5066/P9TLL89E>
- Smith, D. A., Holmes, S. A., Li, X., Guillaume, S., Wang, Y. M., Bürki, B., ... & Damiani, T. M. (2013). Confirming regional 1 cm differential geoid accuracy from airborne gravimetry: the Geoid Slope Validation Survey of 2011. *Journal of geodesy*, 87(10-12), 885-907.
- Wang, Y. M., Huang, J., Jiang, T., & Sideris, M. G. (2016). Local geoid determination. Encyclopedia of geodesy.
- Wang, Y. M., Becker, C., Mader, G., Martin, D., Li, X., Jiang, T., ... & Bürki, B. (2017). The Geoid Slope Validation Survey 2014 and GRAV-D airborne gravity enhanced geoid comparison results in Iowa. *Journal of Geodesy*, 91(10), 1261-1276.
- Wang YM, Sánchez L, Ågren J, Huang J, Forsberg R, Abd-Elmotaal HA, Barzaghi R, Bašić T, Carrion D, Claessens S, Erol B, Erol S, Filmer M, Grigoriadis VN, Isik MS, Jiang T, Koç Ö, Li X, Ahlgren K, Krcmaric J, Liu Q, Matsuo K, Natsiopoulos DA, Novák P, Pail R, Pitoňák M, Schmidt M, Varga M, Vergos GS, Véronneau M, Willberg M, Zingerle P (2021) Colorado geoid computation experiment—overview and summary, *J Geod. Special Issue on Reference Systems in Physical Geodesy*
- van Westrum, D., Ahlgren, K., Hirt, C., Guillaume S. (2021) A Geoid Slope Validation Survey in the rugged terrain of Colorado, USA. *Journal of Geodesy*, 95(9). <https://doi.org/10.1007/s00190-020-01463-8>

## BIOGRAPHICAL NOTES

Kevin Ahlgren is a geodesist and geoid modeler within NGS's Observations and Analysis Division. He has a Ph.D. in Geodetic Science and Surveying from the Ohio State University.

## CONTACTS

Dr. Kevin M. Ahlgren  
National Oceanic and Atmospheric Administration – National Geodetic Survey  
1315 East West Highway, SSMC3  
Silver Spring, MD  
UNITED STATES  
Tel. +01 240 533 9894  
Email: [kevin.ahlgren@noaa.gov](mailto:kevin.ahlgren@noaa.gov)  
Web site: <https://geodesy.noaa.gov/index.shtml>